

RESEARCH ARTICLE

Open Access



Identification of novel and differentially expressed MicroRNAs in goat enzootic nasal adenocarcinoma

Bin Wang, Ni Ye, San-jie Cao, Xin-tian Wen, Yong Huang and Qi-gui Yan*

Abstract

Background: MicroRNAs (miRNAs) post-transcriptionally regulate a variety of genes involved in eukaryotic cell growth, development, metabolism and other biological processes, and numerous miRNAs are implicated in the initiation and progression of cancer. Enzootic nasal adenocarcinoma (ENA), an epithelial tumor induced in goats and sheep by enzootic nasal tumor virus (ENTV), is a chronic, progressive, contact transmitted disease.

Methods: In this work, small RNA Illumina high-throughput sequencing was used to construct a goat nasal miRNA library. This study aimed to identify novel and differentially expressed miRNAs in the tumor and para-carcinoma nasal tissues of Nanjiang yellow goats with ENA.

Results: Four hundred six known miRNAs and 29 novel miRNAs were identified. A total of 116 miRNAs were significantly differentially expressed in para-carcinoma nasal tissues and ENA (54 downregulated; 60 upregulated; two only expressed in control group); Target gene prediction and functional analysis revealed that 6176 non-redundancy target genes, 1792 significant GO and 97 significant KEGG pathway for 121 miRNAs (116 significant expression miRNAs and five star sequence) were predicted. GO and KEGG pathway analysis revealed the majority of target genes in ENA are involved in cell proliferation, signal transduction and other processes associated with cancer.

Conclusions: This is the first large-scale identification of miRNAs in *Capra hircus* ENA and provides a theoretical basis for investigating the complicated miRNA-mediated regulatory networks involved in the pathogenesis and progression of ENA.

Keywords: MicroRNA, Enzootic nasal adenocarcinoma, Illumina high-throughput sequencing, Gene ontology, KEGG pathway

Background

MicroRNAs (miRNAs) are endogenous, 21–24 nucleotide-long, non-coding RNAs that regulate gene expression in eukaryotes; however, some viruses also express miRNAs in host cells [1–3]. MiRNAs are complementary to specific sequence motifs in the 3' untranslated regions (UTRs) of their target mRNAs and negatively regulate gene expression at the post-transcriptional level by inhibiting translation or promoting mRNA degradation, based on the degree of complementary base pairing between the miRNA and mRNA. MiRNAs regulate approximately 30 % of genes

in higher eukaryotic cells, including genes involved in development, metabolism, apoptosis, proliferation and viral defense [4–10]. The earliest evidence for an association between miRNAs and cancer came from the study of chronic lymphocytic leukemia (CLL) [11]. To date, more than 50 % of miRNAs have been shown to be encoded in chromosome fragile sites that are often absent, amplified or rearranged in malignant tumor cells leading to dysregulated expression of miRNAs, and numerous miRNAs have been shown to play important roles in tumorigenesis [12, 13]. MiRNAs can act in a similar manner to oncogenes or tumor suppressor genes and have emerged as a novel type of regulatory factor in the epigenetic modification of gene expression. According to predictions in vertebrates, a single miRNA can regulate more than 400 target genes,

* Correspondence: yanqigui@126.com
Ni Ye as the joint first author.

College of Veterinary Medicine, Sichuan Agricultural University, Hui Min Road 211, Chengdu, Sichuan 611130, People's Republic of China



forming complicated regulatory networks [14–23]. Therefore, miRNAs have become a focus of cancer research in order to identify novel molecular methods for the diagnosis, prognostication and treatment of human cancer. Now researchers can directly obtain miRNA sequences and discover novel miRNAs through utilize Illumina high-throughput sequencing technology [24].

Enzootic nasal adenocarcinoma (ENA) is an epithelial tumor caused by enzootic nasal tumor virus (ENTV), and is a chronic, progressive, contact transmitted disease [25]. With the exception of Australia and New Zealand, this disease has spread throughout goats or sheep almost worldwide [26]. ENA originates from the ethmoid area of the nasal cavity either unilaterally or bilaterally, and the tumors are soft, whitish or pinkish-red in color and can partially or completely obscure the nasal cavity [27]. Metastases to the regional lymph nodes, brain or other organs does not occur [28]. So far, there are no effective methods for early diagnosis of ENA and the goats or sheep can only be culled after symptoms appear. More seriously, as it is difficult to distinguish between animals with a latent infection and healthy animals, the virus spreads within herds, and can infect a large number of goats or sheep and threaten the entire population.

There are currently 2581 human mature miRNAs in the miRbase (v21) database; however, there is no public miRNA library of *Capra hircus* nasal tissues and there have been no reports of miRNAs in ENA. To further complicate matters, attempts to establish a system of cultivating ENTV in vitro have failed, which presents a significant obstacle to investigating the immunological characteristics of ENTV and the mechanisms by which it promotes tumorigenesis [29]. Therefore, taking advantage of knowledge of the roles of miRNAs in human cancer to research the miRNAs involved in ENA may not only avoid the problem of cultivating ENTV in vitro, but also shifts the focus to the cells targeted by ENTV - goat or sheep nasal epithelial cells - and may provide an alternative method for investigating the tumorigenic effects of ENTV.

Using Illumina high-throughput sequencing technology to detect miRNAs expressed in the tumor and para-carcinoma nasal tissues of Nanjiang yellow goats with ENA, we constructed the first goat nasal tissue miRNA library. Furthermore, the target genes of the differentially expressed miRNAs in ENA were predicted and their corresponding biological functions were analyzed. This research may help to identify novel biomarkers for ENA, lays a foundation for investigating the mechanism by which ENTV promotes tumorigenesis, and provides further information on the role of miRNAs in cancer. Furthermore, as the sequences and roles of miRNAs are well conserved, the findings of this study may also be relevant to human cancers such as nasopharyngeal carcinoma.

Methods

Animals and tissue samples

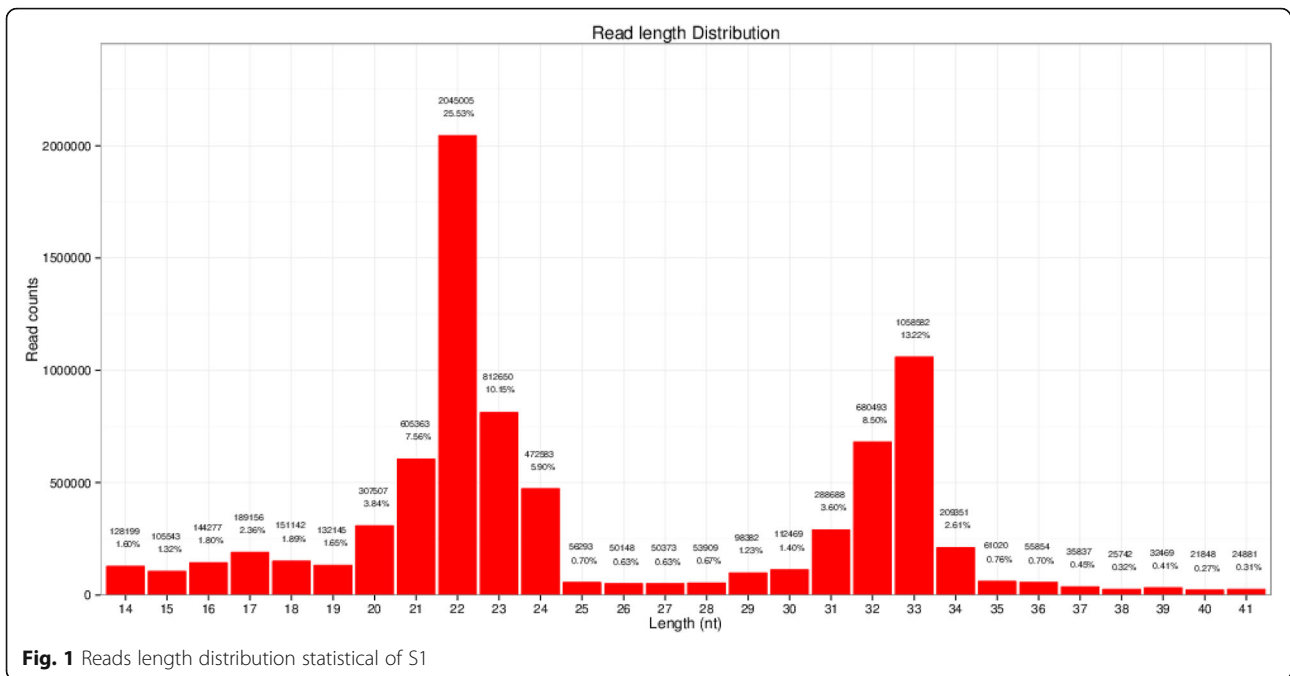
Eight goats (3a-4a, Nanjiang Yellow Goat) infected by ENTV under natural conditions at a farm in Sichuan were quarantined and transported to Sichuan Agricultural University laboratory animal center, and grew up the center. After slaughter, tumor and para-carcinoma nasal tissues were collected, frozen rapidly in liquid nitrogen and stored at -80°C . After pathological analysis, the samples from three Nanjiang yellow goats whose nasal passages were unilaterally blocked by tumors were selected for high-throughput sequencing. The nasal tumors in these animals were poorly differentiated (i.e., at the same state of differentiation) with no tumor cell infiltration in the matched para-carcinoma tissues.

Preparation of samples for sequencing and qPCR

Samples of cDNA from the tumor tissues (numbers S1, S3, S5) and matched para-carcinoma tissues (numbers S2, S4, S6) of the three animals described above were shipped on dry ice to Jing Neng Bio-Technology corporation (Shanghai, China) for high-throughput sequencing. Briefly, total RNA was extracted from the tissues using RNazol RT RNA Isolation Reagent (GeneCopoela, Rockville, MD, USA) according to the manufacturer's protocol. The RNA concentrations were determined using a Smart Specplus Spectrophotometer (Bio-Rad, Hercules, CA, USA) and the integrity of the total RNA samples was verified by polyacrylamide gel electrophoresis (PAGE). The All-In-One miRNA qRT-PCR Detection Kit (GeneCopoela) was used to add poly(A) tails to the miRNAs in the total RNA samples and M-MLV reverse transcriptase was used to synthesize cDNA according to the manufacturer's instructions. Each reaction mixture contained 5 μL of 5x reaction buffer, 1 μL RTase Mix, 1 μL of 2.5 U/ μL PolyA Polymerase, 2 μg total RNA and RNase-/DNase-free H₂O to 25 μL , and was incubated at 37 $^{\circ}\text{C}$ for 1 h and then at 85 $^{\circ}\text{C}$ for 5 min to inactivate the enzyme.

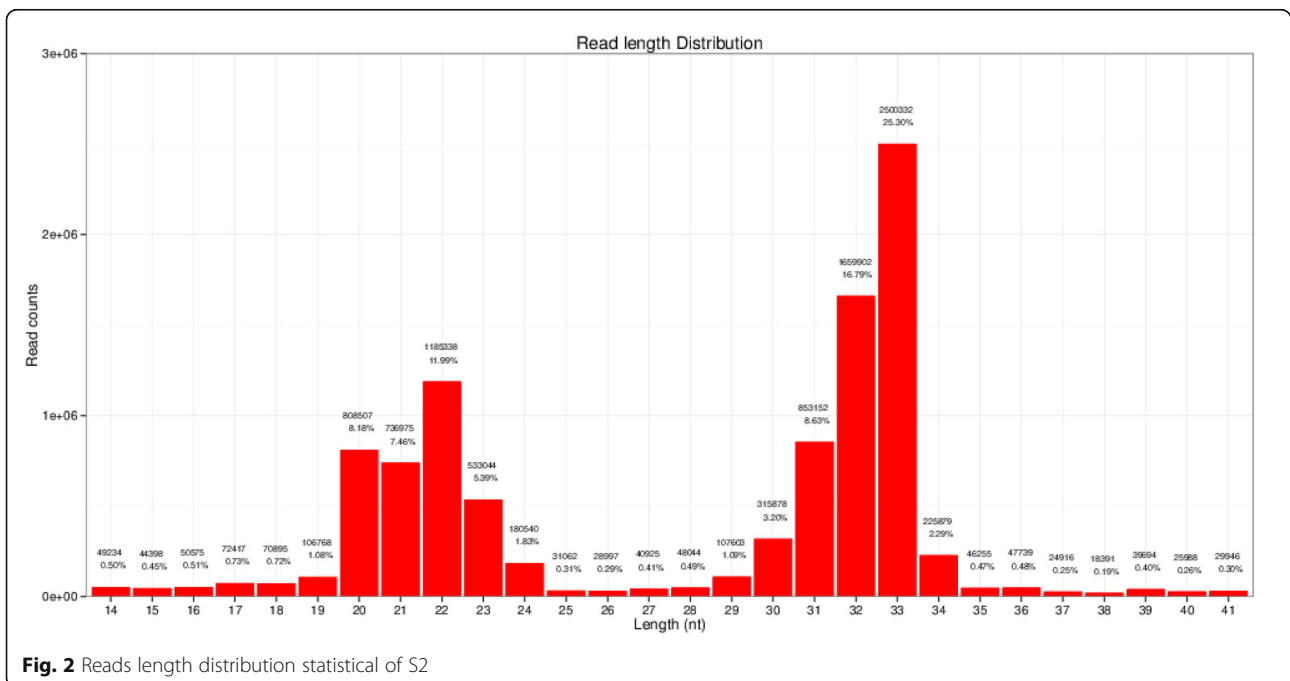
Analysis of sequence data and creation of miRNA library

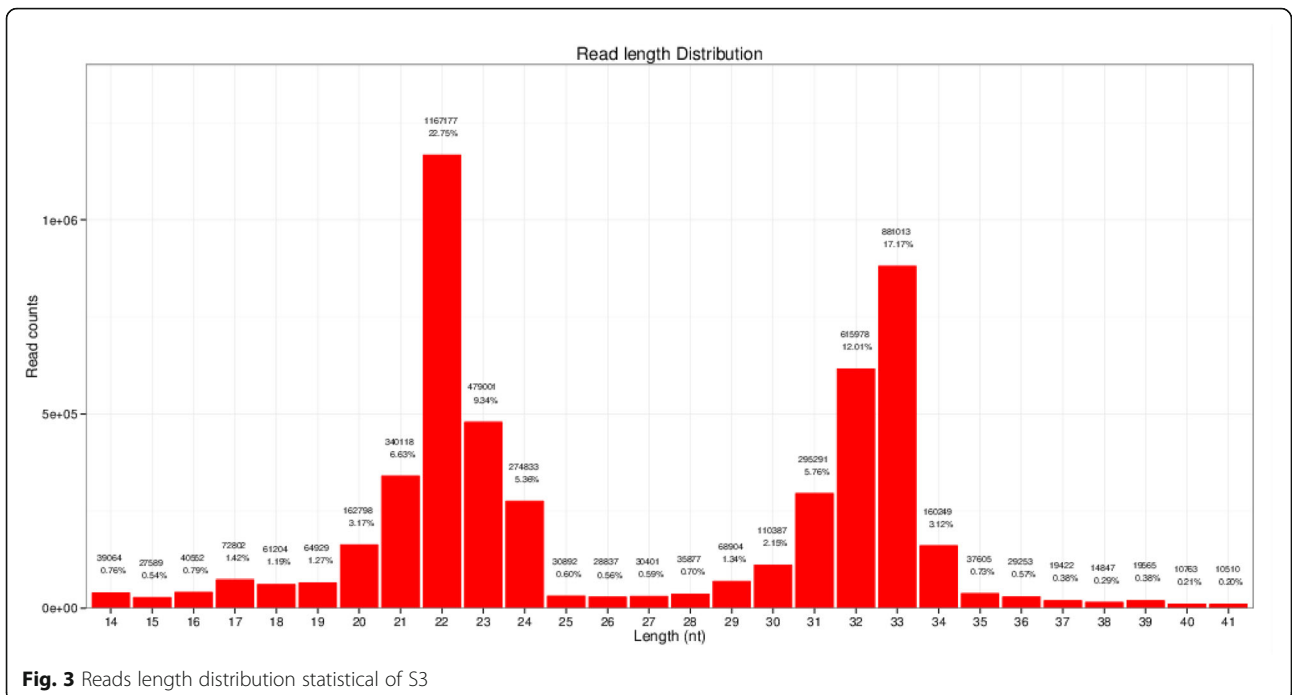
Single-read 50 bp sequencing was adopted for high-throughput sequencing. Illumina CASAVA software was used to convert the original data image files into sequence files, and FastQC statistical software was used to evaluate the quality of the data. Primer, adaptor and low quality sequences were excluded and 15–40 base sequences meeting the length and quality requirements were selected as clean reads of reliable quality for further analysis (Figs. 1, 2, 3, 4, 5 and 6). Total clean reads from each individual sample were aligned with the *Capra hircus* genome in NCBI (ftp://ftp.ncbi.nlm.nih.gov/genomes/Capra_hircus) using Bowtie software [30] (<http://bowtie-bio.sourceforge.net/index.shtml>), and then blasted against



the Rfam (<http://www.sanger.ac.uk/resources/databases/rfam.html>), RepBase (<http://www.girinst.org/repbase/>), EST (<http://www.ncbi.nlm.nih.gov/nucest/>) and miRBase (<http://www.mirbase.org/>) databases. Sequence alignment was set to allow only a single base mismatch, and the results were sorted in the order of known miRNAs > rRNAs >

tRNAs > snRNAs > snoRNAs > repeat, respectively, which enabled each small RNA to obtain a unique annotation. The remaining sequences were mapped to Denovo prediction data sets [31] and the *Capra hircus* genome to exclude known non-miRNA sequences (such as tRNAs, rRNAs, snRNAs and snoRNAs) and identify novel miRNAs.



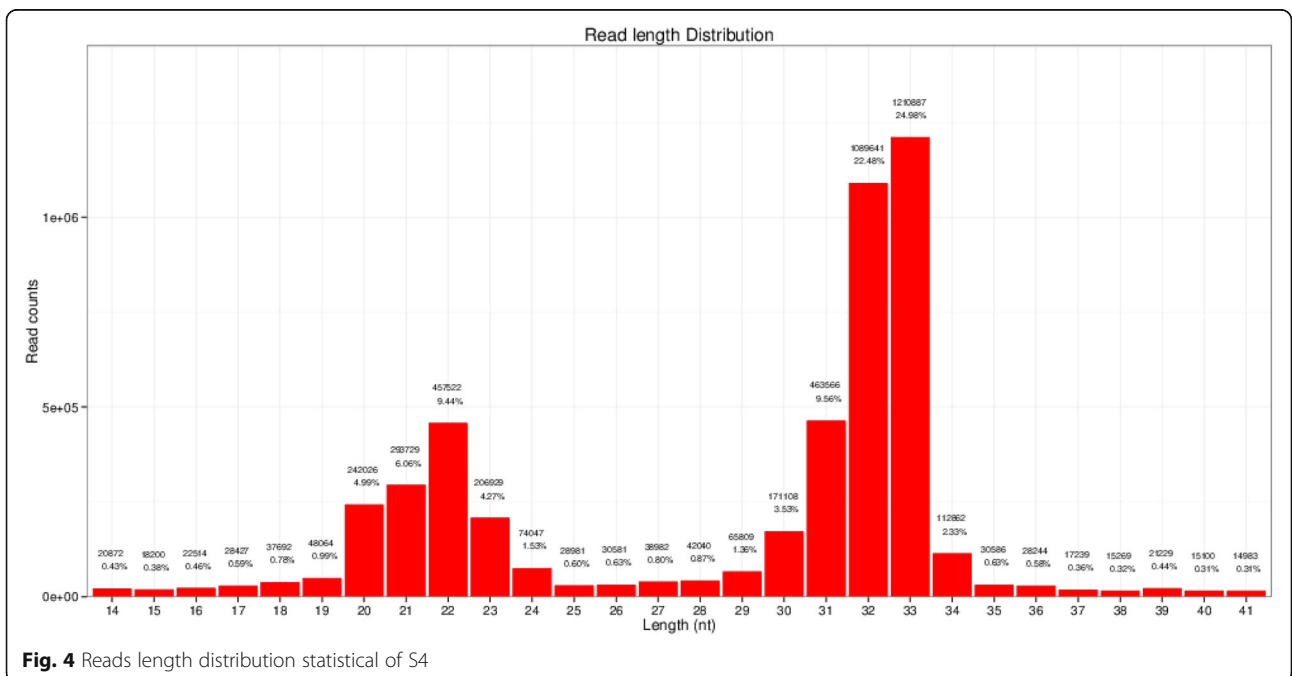


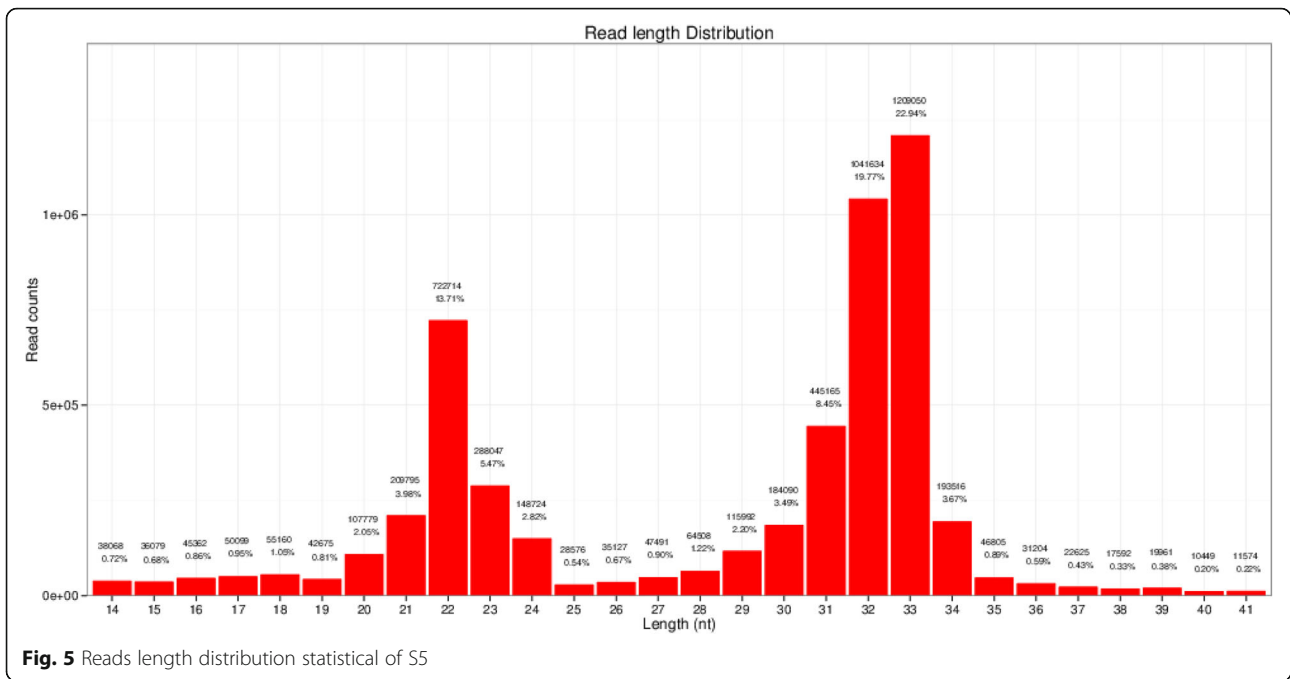
MiRDeep [32] and RNAfold [33] were used to predict miRNA precursor sequences, star miRNAs and mature miRNAs, and then the energetic stability, position and read frequencies for each potential miRNA precursor were computed using miRDeep according to the compatibility of energetic stability, positions, frequencies of reads. Ultimately, a *Capra hircus* nasal tissue miRNA library was

created by combining the sequencing data from all six samples.

Identification of differentially expressed miRNAs in ENA

The sequences in each sample were compared with the miRNA library established in this study by assessing the numbers of transcripts per million (TPM). TPM was



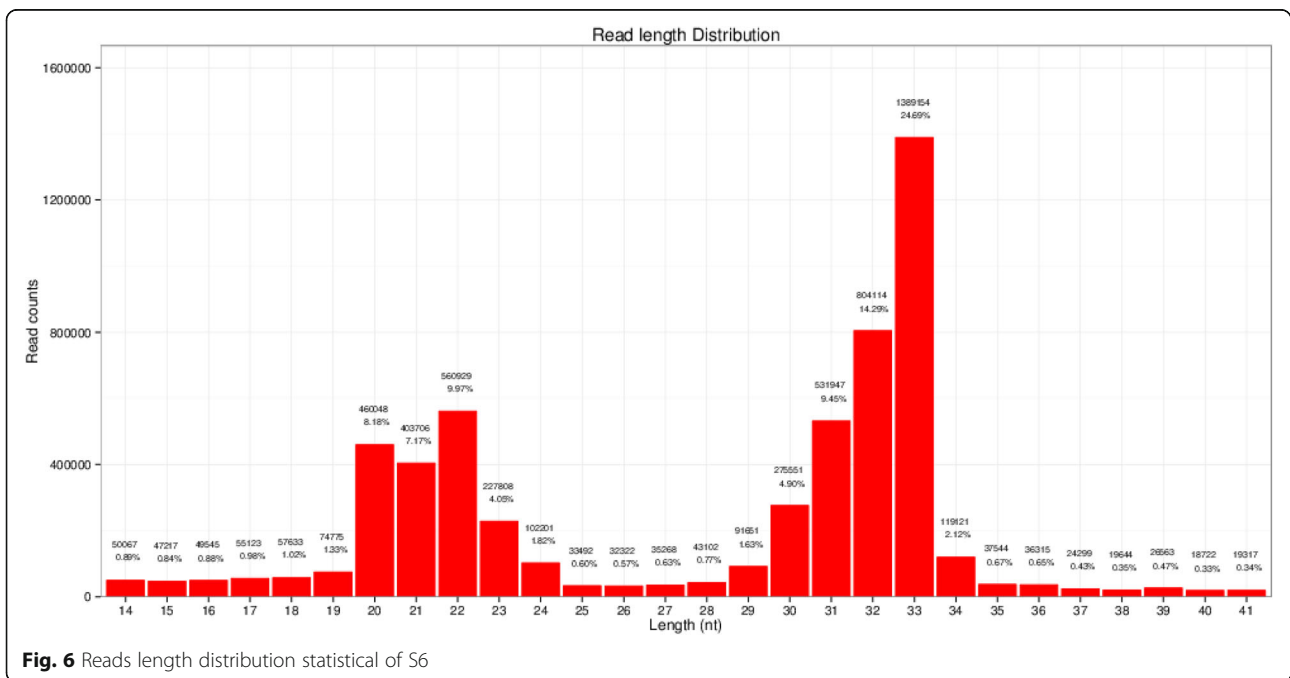


calculated as (numbers of each miRNA matched to total reads)/(number total reads) × 10⁶. TPM is an indicator of the quantity of miRNA expression per million match paired sequences. The total numbers of matched pair reads were used in the normalized numerical expression algorithm to calculate miRNA expression. DESeq [34] software was used to identify differentially expressed miRNAs between the para-carcinoma tissues (S2, S4, S6)

and ENA (S1, S3, S5) on the basis of a fold-change greater than or equal to two and *P*-value ≤ 0.05.

Prediction and analysis of miRNA target genes

The Miranda algorithm [35] was used to predict the target genes of the miRNAs that were differentially expressed in ENA. The threshold parameters for predicting miRNA target genes were a total score ≥150, Δ*G* ≤ -30 kcal/mol,



and strict 5' seed pairing. The pathways these candidate target genes are involved in was analyzed by functional annotation utilizing the NCBI, KEGG (<http://www.genome.jp/kegg/>) [36] and GO (<http://geneontology.org/>) [37] databases. Additionally, high-throughput sequencing allowed the mRNA expression of all of the potential target genes to be analyzed in the same samples (data not shown); therefore, GO and KEGG analyses could be conducted on the differentially expressed target genes of the differentially expressed miRNAs. GO annotation and enrichment analysis was performed for three gene ontologies: molecular function, cellular components and biological processes. The following formula was used to calculate the P -values:

$$P = 1 - \sum_{i=0}^{m-1} \frac{\binom{M}{i} \binom{N-M}{n-i}}{\binom{N}{n}}$$

where N is the number of genes with GO/KEGG annotations; n is the number of target gene candidates in N ; M is the number of genes that annotated to a certain GO term/pathway, and m is the number of target gene candidates in M . GO terms and KEGG pathways with a corrected P -value ≤ 0.5 were regarded as significantly enriched.

Validation of the expression of key differentially expressed miRNAs

Key miRNAs that were identified in all of the analyses described above were quantified in ENA and para-carcinoma tissue samples from five goats with ENA whose nasal passages were unilaterally blocked by tumors. Total RNA was isolated and reverse transcribed as described above, then the cDNA products were diluted 5-fold with sterile H₂O and subjected to quantitative real-time PCR (qPCR) using the All-In-One miRNA qRT-PCR Detection Kit (GeneCopoela) with U6 snRNA and *GAPDH* as internal references. Each reaction contained 10 μ L of 2x All-in-One qPCR Mix, 2 μ L All-in-One miRNA qPCR Primer (2 μ M; prepared by Life Technologies, Shanghai, China), 2 μ L Universal Adaptor qPCR Primer (2 μ M), 2 μ L first-strand cDNA and 4 μ L double distilled water. The cycling conditions were 95 °C for 10 min, 40 cycles of 95 °C for 10 s, 60 °C for 20 s and 72 °C for 20 s, followed by melting curve analysis. Relative quantification was performed using the $2^{-\Delta\Delta C_t}$ method [38], and t -tests were used to examine the significance of the differences in expression between the para-carcinoma tissues and ENA.

Results

Capra hircus nasal tissue miRNA library

High-throughput sequencing generated hundreds of millions of reads for each tissue. The raw data (tag

sequences and counts) have been submitted to Gene Expression Omnibus (GEO) under series GSE65305. To estimate sequencing quality, the quality scores were analyzed across all bases (Fig. 7). The lowest quality score was ≥ 30 ; therefore, the error rate was lower than 0.1 %. Reads including adaptor sequences, low quality sequences and sequences of unqualified length were removed, and the remaining clean reads were aligned with the *Capra hircus* genome in NCBI using Bowtie software to analyze the genomic distribution and expression of small RNAs. The vast majority of clean reads (at least 84.75 %) and unique reads (at least 57.56 %) mapped to the *Capra hircus* genome (Table 1).

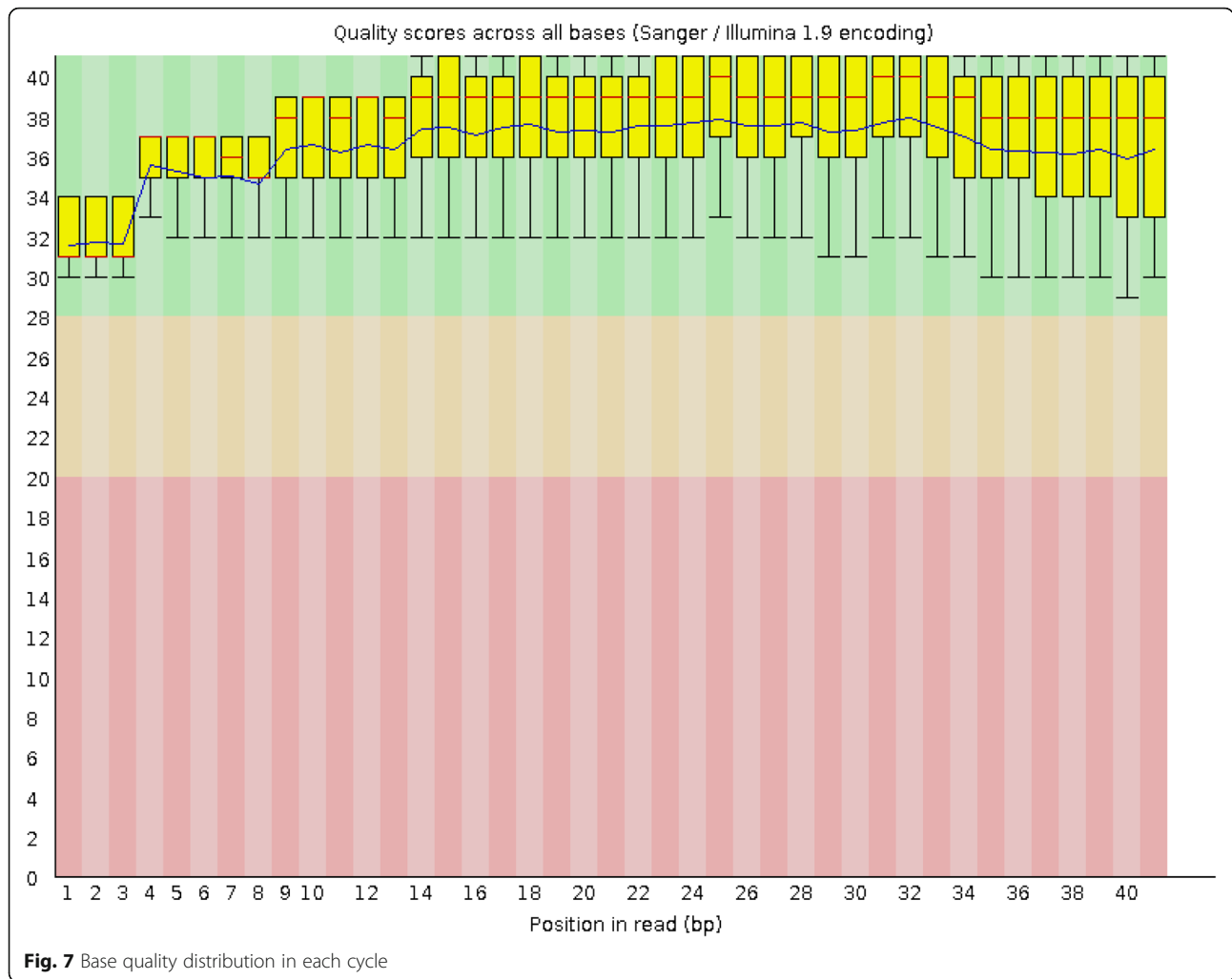
Unique reads were blasted against the Rfam, RepBase, EST and miRBase databases, in the order of known miRNAs > rRNAs > tRNAs > snRNAs > snoRNAs > repeat sequences, which enabled each small RNA obtain a unique annotation. To exclude other RNAs, such as tRNAs, rRNAs, snRNAs and snoRNAs, the remaining sequences were mapped to Denovo prediction data sets and the *Capra hircus* genome to identify novel miRNAs. miRDeep prediction [32] and RNAfold [33] software were used to analyze secondary structure. A total of 435 sequences (29 novel miRNAs) were included in the miRNA library. Additional file 1: Table S1 displays the sequencing generated codes and corresponding *Capra hircus* miRNAs or novel miRNA_id. As research into miRNAs in human cancer is widespread, we blasted all goat miRNAs against the human miRNAs in miRBase v21 to further understand their function. A total of 615 of the goat miRNAs had analogues in the human miRNA datasets (Additional file 2: Table S2).

Identification of differentially expressed miRNAs in ENA

A total of 435 miRNAs were identified in the ENA and para-carcinoma tissues. The Additional file 3: Table S3 lists the expression of all miRNAs. The expression of 116 miRNAs was significantly different in para-carcinoma tissues and ENA, of which 54 were downregulated and 60 were upregulated in ENA. In addition, 2 miRNAs were only expressed in the para-carcinoma tissues (Additional file 4: Table S4). The majority of the fold change- \log^2 values ranged from 1 to 5.42; chi-miR-133a-3p had the highest fold-change- \log^2 of at least 5.4-fold, and 65 miRNAs had fold-change- \log^2 values of at least two-fold. Figure 8 indicates the differences in expression of all 435 miRNAs between ENA and the para-carcinoma tissues.

Functional analysis of differentially expressed target genes regulated by differentially expressed miRNAs

The Miranda algorithm indicated thousands of potential target genes for the 435 miRNAs. According to the total scores and predicted energies, the 6176 non-redundancy target genes of these 121 miRNA (116 significant



expression miRNAs and five star miRNAs) were selected, reflecting 15222 corresponding relationships between the differentially expressed miRNAs and their target genes. Additional file 5: Table S5 shows the total stores, total energy, and protein-id and genomic location of predicted target genes.

The expression of these candidate target genes was assessed in the high throughput sequencing data obtained from the same ENA and para-cancerous tissue samples

(data not shown; this data will be described in another article). A total of 175 mRNAs that were significantly differentially expressed in ENA were selected for this analysis. Additional file 6: Table S6 lists the differentially expressed miRNAs and their corresponding differentially expressed target genes. Additional file 7: Table S7 summarizes the degree of regulation between the differentially expressed miRNAs and their differentially expressed target mRNAs.

Table 1 The results of clean reads and unique reads mapped to the Capra Hircus genome in cancer and control groups

Samples	Clean reads	Total aligned reads	Total aligned reads (%)	Total unaligned reads	Total unaligned reads (%)	Unique reads	Unique aligned reads	Unique aligned reads (%)	Unique unaligned reads	Unique unaligned reads (%)
S1	8009909	7174638	89.57	835271	10.43	335710	239081	71.22	96629	28.78
S2	9883394	8614567	87.16	1268827	12.84	236291	149260	63.17	87031	36.83
S3	5129861	4573796	89.16	556065	10.84	204228	127183	62.28	77045	37.72
S4	4847129	4108137	84.75	738992	15.25	203603	117200	57.56	86403	42.44
S5	5269861	4598556	87.26	671305	12.74	231658	154306	66.61	77352	33.39
S6	5627178	4846400	86.12	780778	13.88	225210	143168	63.57	82042	36.43

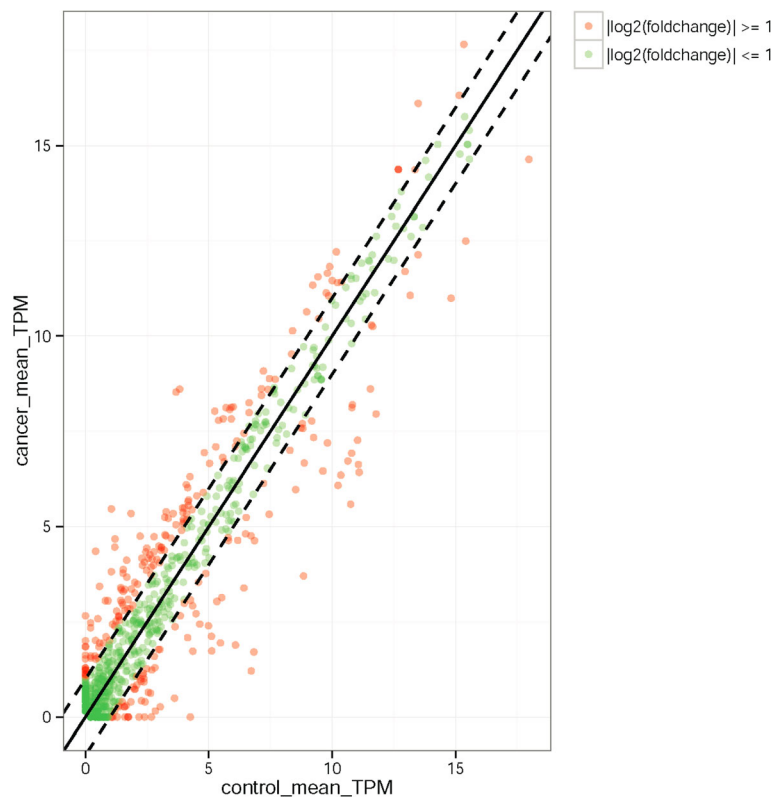


Fig. 8 Relative expression of miRNAs in ENA and para-cancerous tissues. The x- and y-axes indicate the mean TPM expression levels of the miRNAs in each tissue. The red circles represent miRNAs with a fold change ≥ 2 ; green circles represent miRNAs with a fold change ≤ 2 ; the points on the dotted line represent miRNAs with a fold change = 2. Fold changes were calculated as the mean miRNA TPM in ENA/mean miRNA TPM in para-cancerous tissues

MiRNA-gene ontology network analysis of miRNA target genes

Functional analysis was conducted on the mRNAs predicted as targets of the 435 differentially expressed miRNAs. A total of 9777 GO enrichments were identified, of which 1792 GO categories were significant ($P \leq 0.05$). The mRNA sequencing identified a total of 90 target genes corresponding to miRNAs with significantly decreased expression and 84 target genes corresponding to miRNA with significantly increased expression in tumor group. Four hundred seventy-two significant GO enrichments exist in significant expression miRNA-mRNA network (Additional file 8: Table S8). The target genes of the differentially expressed miRNAs were mainly involved in cell differentiation, MAP kinase activity, cell adhesion and angiogenesis; each of these pathways may be implicated in the tumorigenic effect of ENTV. Figure 9 presents the ten most-enriched GO categories for the differentially expressed target genes of the differentially expressed miRNAs in ENA.

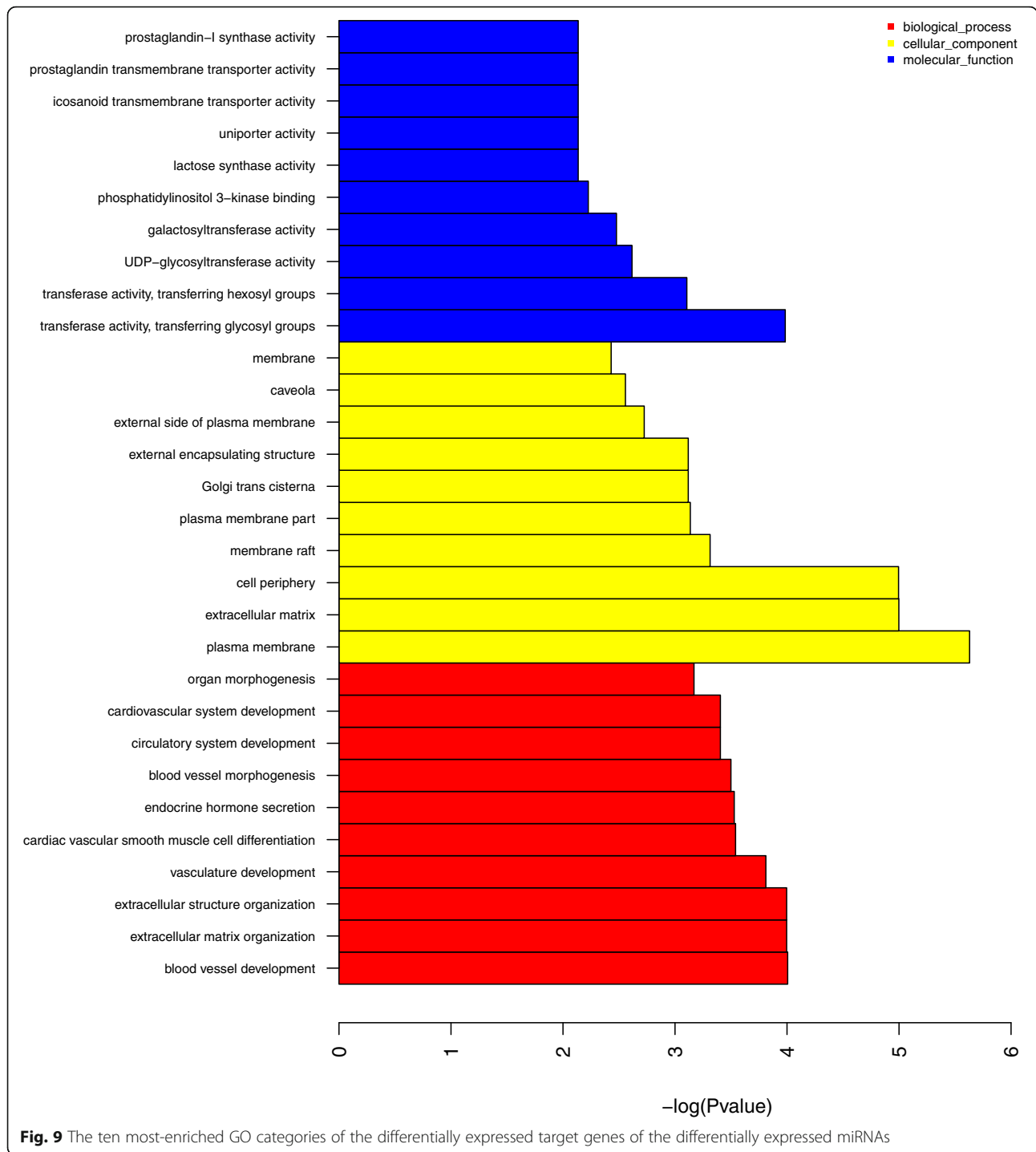
Analysis of signaling pathways regulated by the miRNA target genes

Signal transduction analysis was conducted on the mRNAs predicted as targets of the 435 differentially expressed

miRNAs, and 267 KEGG enrichments were identified of which 97 were significant ($P \leq 0.05$). The target genes of the differentially expressed miRNAs participate in pathways related to the signal transduction, specific types of cancer and immune system. Among significantly differently expressed miRNA, miRNA with increased expression in tumor group were involved in 83 significant signal transduction pathways (Additional file 9: Table S9), miRNA with reduced expression in tumor group were involved in 89 significant signal transduction pathways (Additional file 10: Table S10). Figure 10 illustrates the ten most-enriched KEGG pathways for the differentially expressed target genes of the differentially expressed miRNAs in ENA.

Quantitative RT-PCR validation of differentially expressed miRNAs

We selected nine of the key miRNAs that were significantly differently expressed in ENA including five miRNAs that featured in both the GO and KEGG pathway analyses and two novel miRNAs (NW_005102245.1_1433, NC_022308.1_285). The main functions of target genes regulated by these miRNAs are involved in cancer pathogenesis, virus infection, cell apoptosis and proliferation. As shown in Fig. 11, qRT-PCR confirmed the



expression of the nine miRNAs between ENA and the para-cancerous tissues with an increased sample size. The expression trend of eight miRNAs is in accordance with Illumina High-Throughput Sequencing, one miRNA (chi-miR-218) have shown a down-expression in tumor group in sequencing and qPCR verification, but the down-expression multiple is different.

Discussion

ENTV, a betaretrovirus that infects sheep (ENTV-1) and goats (ENTV-2), is associated with neoplastic transformation of ethmoid turbinate epithelial cells and leads to ENA. The clinical symptoms of goats are a loss of appetite, extreme weight loss, dyspnea, rhinorrhea, and unilateral or bilateral nasal puffiness. The incidence of

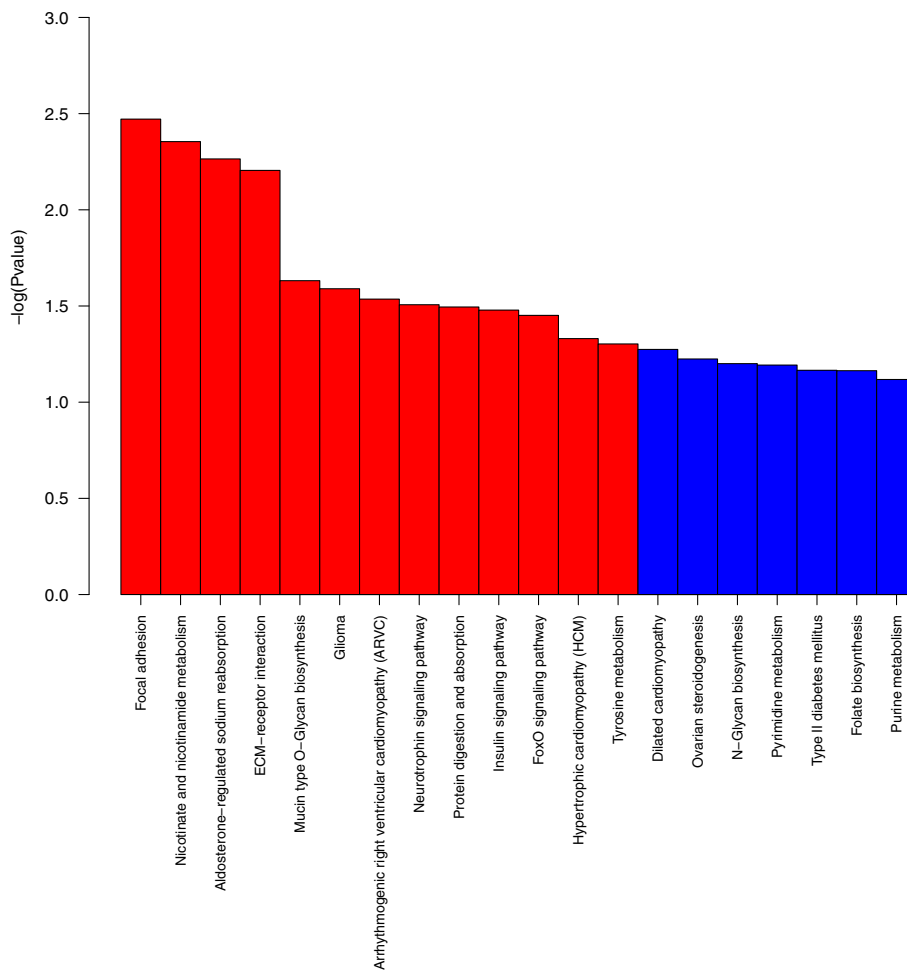


Fig. 10 The ten most-enriched signaling pathways of the differentially expressed target genes of the differentially expressed miRNAs

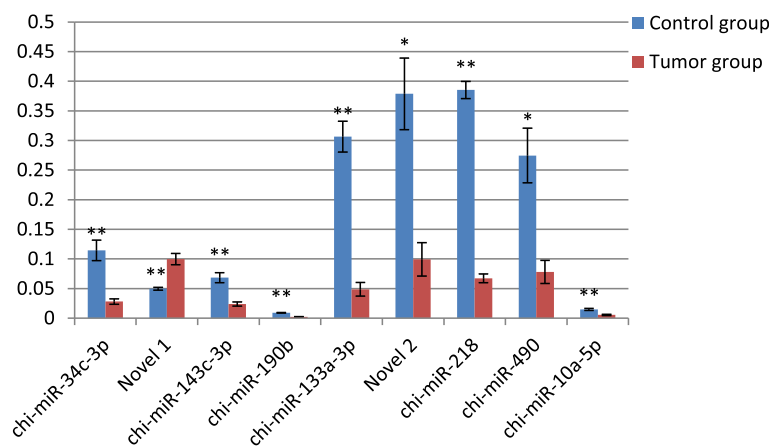


Fig. 11 qRT-PCR validation of the identified miRNAs using Illumina sequencing technology. Real-time RT-PCR analysis of nine miRNAs in the tumour and para-carcinoma tissues from five goats with ENA. Relative quantification was assessed using the $2^{-\Delta\Delta C_t}$ method and was normalized to *U6* and *GAPDH*. $2^{-\Delta\Delta C_t}$ Means \pm SE relative expression levels are presented. * represents $p < 0.05$, ** represents $p < 0.01$

ENTV infection ranges from 5 to 15 %, and once the clinical symptoms of ENA appear, almost all cases are fatal [39–41]. High-throughput sequencing technology is gradually being used in animal and has provided some knowledge of goat miRNAs. Ji et al. [42] discovered 290 known miRNAs and 38 novel miRNAs in dairy goat mammary gland tissue and reported that miRNA-mediated regulation of gene expression occurs during early lactation. Hao et al. [43] found that the expression of 64 miRNAs was reduced in the skin of a 70-day fetus relative to a lamb born at 2 weeks, with the expression of ten miRNAs decreasing more than 5-fold, which implies that miRNAs play an important role in maintaining normal skin function.

Cancer is a leading cause of morbidity and death in humans. Significant research has been conducted on miRNAs in human cancer, and miRNAs have been demonstrated to be directly involved in human nasopharyngeal carcinoma (NPC). For example, miR-29c, the miR-34 family, miR-143, miR-145 and miR-9 are downregulated in NPC, leading to increased expression of their target genes which influence the function and synthesis of extracellular matrix proteins, which in turn affects tumor invasion and metastasis, and activates the TGF-Wnt, IP3 and VEGF signaling pathways [44, 45]. In contrast, miR-200, the miR-17-92 cluster and miR-155 are upregulated in NPC, and miR-200 inhibits the migration and invasion of NPC cells by inhibiting the expression of *ZEB2* (zinc finger E-box binding homeobox 2) and *CTNNB1* (catenin- β -like 1) [46]. By blasting the 435 miRNAs identified using high-throughput sequencing in this study against the human miRNA datasets in miRBase, we found that hsa-miR-9, hsa-miR-34 and hsa-miR-143 are significantly downregulated and hsa-miR-200 is significantly upregulated in ENA. GO and KEGG pathway analysis revealed these miRNAs are involved in intracellular signal transduction, the MAPK cascade and cell morphogenesis, among other processes.

Our study found according to the percentage, the top five signaling pathways are MAPK signaling pathway, Pathways in cancer, PI3K-Akt signaling pathway, Ras signaling pathway and Viral carcinogenesis. Kano et al. [47] and Chiyomaru et al. [48] found that miR-133a was significantly inhibited human esophageal squamous cell cancer and the invasion of bladder cancer cell. Iorio [49] found that expression of miR-133a significantly reduced during the progression of breast cancer. Our results also reveal the expression of miR-133a-3p was at least 5-fold lower in ENA compared to para-carcinoma nasal tissues. These results suggest that miR-133a-3p may regulate the expression of oncogenes and inhibit tumorigenesis. KEGG analysis displayed that the target genes of miR-133a-3p are involved in tumor biology at multiple nodes, such as regulation of cell differentiation, apoptosis, signal transduction and cell

adhesion, invasion and migration. In esophageal squamous cell carcinoma and bladder cancer, miR-133a targets fascin actin-bundling protein 1 (*FSCN1*) to regulate cancer cell invasion, migration and proliferation [47, 49]. However, in this study we identified that serine/threonine-protein kinase B-raf (*BRAF*) as chi- miR-133a-3p, chi-miR-145-5p, chi-miR-146a/200a and two novel miRNA (NC-022308.1-260, NC-022294.1-874) target gene which acts upstream regulatory factor in RAS-RAF-MEK-ERK. Sustained activation of BRAF will lead to cell deterioration and excessive proliferation [50]. In addition, the miR-133a-3p target genes: *MDS1* and *EVII* complex (*MECOM*) may also play a significant role in pathways related to cancer. In chronic myeloid leukemia (*CML*), expression of the oncogene *MECOM* correlates with progression. The tyrosine kinase catalytic activity of the oncoprotein BCL-ABL1 regulates *MECOM* expression, and conversely *MECOM* partially mediates BCR-ABL1 activity [51]; BCR-ABL1 activates the PI3K, MAPK and JAK-STAT signal transduction pathways [52–54] to promote abnormal proliferation, differentiation, transformation and survival in myeloid cells [55]. However, forkhead box O (*FoxO*) as the intersection of PI3K and RAS signaling pathway can inhibit cell proliferation and induce cell cycle stop. The activation of the PI3K signaling pathway inhibits the activity of the FoxO transcription factor [56, 57], which increase the chances of tumor formation. Further study is required to determine if *MECOM* and BCR-ABL1 play a role in the pathogenesis of ENA.

miR-148a is an oncogene that is upregulated in hepatocellular carcinoma cells (*HCC*) and enhances cell proliferation, migration, invasion and stimulates the epithelial to mesenchymal transition (*EMT*) by targeting tumor suppressor gene: phosphatase and tensin homolog (*PTEN*) [58]. However, *PTEN* was not identified as a target of miR-148a in this study. Its predicted targets were the transforming growth factor β receptor associated protein 1 (*TGF β RAP1*) which can specifically combine with the receptor of transforming growth factor β (*TGF β*), and then help to realize the biological function of TGF β [59]. TGF β can inhibit cells growth in malignant tumor such as head and neck squamous cancer, colon cancer, breast cancer [60–62]. The present studies have pointed out that the expression of TGF β in nasopharyngeal phosphorus tumor generally weakened or even disappear, but the adjacent epithelium have stronger expression [63]. The expression of miR-148a-3p was at least 2.5-fold higher in ENA compared to para-carcinoma nasal tissues. Influenced by miR-148-3p expression, *TGF β RAP1* will drop, which will affect the signal pathway of TGF β and make the cancer cell reduction or loss of ability to react to TGF β , finally, the tumor cells escape from negative growth regulation of TGF β . Although this is our speculation, but we believe there is a link between them.

Conclusions

This study provides a solid basis for further research and highlights a number of miRNAs and genes that may be involved in the pathogenesis of ENA. This study of miRNAs in ENA may also provide useful information for basic research into human cancer. In future studies, we aim to confirm the function of the candidate miRNAs in nasal cells. In addition, we hope that these studies may provide some clues to help establish a method for cultivating ENTV *in vitro*.

Additional files

Additional file 1: Table S1. The miRNAs expressed in samples detected by Illumina sequencing. (XLSX 39 kb)

Additional file 2: Table S2. Blast results of all miRNAs against human miRNAs in miRBase v21. (XLSX 152 kb)

Additional file 3: Table S3. The expression of miRNAs in ENA and para-cancerous tissues. (XLSX 171 kb)

Additional file 4: Table S4. Significantly differentially expressed miRNAs in ENA. Positive FoldChange_Log2 indicates upregulation in ENA relative to the para-cancerous tissues; a negative FoldChange_Log2 indicates downregulation in ENA relative to the para-cancerous tissues; inf indicates no expression in para-cancerous tissues; -inf indicates no expression in ENA. (XLSX 30 kb)

Additional file 5: Table S5. Predicted target genes of the differentially expressed miRNAs in ENA. (XLSX 2391 kb)

Additional file 6: Table S6. Differentially expressed miRNAs and their differentially expressed target genes in ENA. (XLSX 30 kb)

Additional file 7: Table S7. Node attributes of the differentially expressed miRNAs and their differentially expressed target genes in ENA. (XLSX 13 kb)

Additional file 8: Table S8. Significantly enriched gene ontology categories the differentially expressed target genes of the differentially expressed miRNAs. (XLSX 85 kb)

Additional file 9: Table S9. Significantly enriched signaling pathways (m = 83) of gene targets of the significantly increased miRNAs in ENA. (XLSX 34 kb)

Additional file 10: Table S10. Significantly enriched signaling pathways (m = 89) of gene targets of the significantly reduced miRNAs in ENA. (XLSX 34 kb)

Abbreviations

CLL: Chronic lymphocytic leukemia; ENA: Enzootic nasal adenocarcinoma; ENTV: Enzootic nasal tumor virus; GAPDH: Glyceraldehyde-3-phosphate dehydrogenase; GEO: Gene expression omnibus; GO: Gene ontology; KEGG: Kyoto encyclopedia of genes and genomes; miRNAs: MicroRNAs; NPC: Nasopharyngeal carcinoma; PAGE: Polyacrylamide gel electrophoresis; qPCR: Quantitative real-time PCR; RNA: Ribonucleic acid; rRNAs: Ribosomal RNAs; snoRNAs: Small nucleolar RNAs; snRNAs: Small nuclear RNAs; TPM: Transcripts per million; tRNAs: Transfer RNAs; UTRs: Untranslated regions

Acknowledgments

The skillful technical assistance of Shanghai Genergy Bio-Corporation is gratefully acknowledged.

Availability of data and material

The raw data (tag sequences and counts) have been submitted to Gene Expression Omnibus (GEO) under series GSE65305.

Authors' contributions

All authors have read and approved of the submission of the manuscript. Conceived and designed the experiments: YQG CSJ WXT. Performed the experiments: WB YE. Analyzed the data: WB YE HY. Contributed reagents/materials/analysis tools: YQG WB YE. Wrote the paper: WB YN.

Competing interest

The authors declare that they have no competing interests.

Ethics approval

This study was carried out in strict accordance with the Guidelines for Experimental Animals of the Ministry of Science and Technology (revised in 2004; Beijing, China) and was approved by the Institutional Animal Care and Use Ethics Committee of Sichuan Agricultural University, NO. SYXK (Chuan) 2014-187.

Received: 14 May 2016 Accepted: 1 November 2016

Published online: 08 November 2016

References

- Bartel DP. MicroRNAs: genomics, biogenesis, mechanism, and function. *Cell*. 2004;116(2):281–97.
- Filipowicz W, Jaskiewicz L, Kolb FA, Pillai RS. Post-transcriptional gene silencing by siRNAs and miRNAs. *Curr Opin Struct Biol*. 2005;15(3):331–41.
- Pfeffer S, Zavolan M, Grässer FA, Chien M, Russo JJ, Ju J, John B, Enright AJ, Marks D, Sander C. Identification of virus-encoded microRNAs. *Science*. 2004;304(5671):734–6.
- Lin MV, King LY, Chung RT. Hepatitis C virus-associated cancer. *Annu Rev Pathol: Mech Dis*. 2015;10:345–70.
- Zhang X-D, Wang Y, Ye L-H. Hepatitis B virus X protein accelerates the development of hepatoma. *Cancer Biol Med*. 2014;11(3):182–90.
- Zhang X, Daucher M, Armistead D, Russell R, Kottitil S. MicroRNA expression profiling in HCV-infected human hepatoma cells identifies potential anti-viral targets induced by interferon- α . *PLoS One*. 2013;8(2):e55733.
- Kincaid RP, Sullivan CS. Virus-encoded microRNAs: an overview and a look to the future. *PLoS Pathog*. 2012;8(12):e1003018.
- Wang M, Kaufman RJ. The impact of the endoplasmic reticulum protein-folding environment on cancer development. *Nat Rev Cancer*. 2014;14(9):581–97.
- Dong H, Lei J, Ding L, Wen Y, Ju H, Zhang X. MicroRNA: function, detection, and bioanalysis. *Chem Rev*. 2013;113(8):6207–33.
- Bandiera S, Pfeffer S, Baumert TF, Zeisel MB. miR-122—a key factor and therapeutic target in liver disease. *J Hepatol*. 2015;62(2):448–57.
- Calin GA, Dumitru CD, Shimizu M, Bichi R, Zupo S, Noch E, Aldler H, Rattan S, Keating M, Rai K. Frequent deletions and down-regulation of micro-RNA genes miR15 and miR16 at 13q14 in chronic lymphocytic leukemia. *Proc Natl Acad Sci*. 2002;99(24):15524–9.
- Calin GA, Sevignani C, Dumitru CD, Hyslop T, Noch E, Yendamuri S, Shimizu M, Rattan S, Bullrich F, Negrini M. Human microRNA genes are frequently located at fragile sites and genomic regions involved in cancers. *Proc Natl Acad Sci U S A*. 2004;101(9):2999–3004.
- Lagana A, Russo F, Sismeiro C, Giugno R, Pulvirenti A, Ferro A. Variability in the incidence of miRNAs and genes in fragile sites and the role of repeats and CpG islands in the distribution of genetic material. *PLoS One*. 2010;5(6):e11166.
- Lewis BP, Shih I-H, Jones-Rhoades MW, Bartel DP, Burge CB. Prediction of mammalian microRNA targets. *Cell*. 2003;115(7):787–98.
- Bartel DP. MicroRNAs: target recognition and regulatory functions. *Cell*. 2009;136(2):215–33.
- Ruby JG, Stark A, Johnston WK, Kellis M, Bartel DP, Lai EC. Evolution, biogenesis, expression, and target predictions of a substantially expanded set of *Drosophila* microRNAs. *Genome Res*. 2007;17(12):1850–64.
- Landgraf P, Rusu M, Sheridan R, Sewer A, Iovino N, Aravin A, Pfeffer S, Rice A, Kamphorst AO, Landthaler M. A mammalian microRNA expression atlas based on small RNA library sequencing. *Cell*. 2007;129(7):1401–14.
- Agarwal V, Bell GW, Nam J-W, Bartel DP. Predicting effective microRNA target sites in mammalian mRNAs. *Elife*. 2015;4:e05005.
- Paraskevopoulou MD, Vlachos IS, Hatzigeorgiou AG. DIANA-TarBase and DIANA Suite Tools: Studying Experimentally Supported microRNA Targets. *Curr Protoc Bioinformatics*. 2016;55:12.14. 11–8.
- Vlachos IS, Zagganas K, Paraskevopoulou MD, Georgakilas G, Karagkouni D, Vergoulis T, Dalamagas T, Hatzigeorgiou AG. DIANA-miRPath v3.0: deciphering microRNA function with experimental support. *Nucleic Acids Res*. 2015;43:W460–6.
- Bertoli G, Cava C, Castiglioni I. MicroRNAs: new biomarkers for diagnosis, prognosis, therapy prediction and therapeutic tools for breast cancer. *Theranostics*. 2015;5(10):1122.

22. Gong J, Liu C, Liu W, Wu Y, Ma Z, Chen H, Guo A-Y. An update of miRNASNP database for better SNP selection by GWAS data, miRNA expression and online tools. *Database*. 2015;2015:bav029.
23. Chou C-H, Chang N-W, Shrestha S, Hsu S-D, Lin Y-L, Lee W-H, Yang C-D, Hong H-C, Wei T-Y, Tu S-J. miRTarBase 2016: updates to the experimentally validated miRNA-target interactions database. *Nucleic Acids Res*. 2016;44(D1):D239–47.
24. Ye L, Su X, Wu Z, Zheng X, Wang J, Zi C, Zhu G, Wu S, Bao W. Analysis of differential miRNA expression in the duodenum of *Escherichia coli* F18-sensitive and-resistant weaned piglets. *PLoS One*. 2012;7(8):e43741.
25. Heras M, Ortin A, Cousens C, Minguñon E, Sharp J. Enzootic nasal adenocarcinoma of sheep and goats. *Curr Top Microbiol Immunol*. 2003;275:201–23.
26. Kawasako K, Okamoto M, Kurosawa T, Nakade T, Kirisawa R, Miyashou T, Komine M, Go T, Imazu S, Takeuchi N. Enzootic intranasal tumour virus infection in apparently healthy sheep in Japan. *Vet Rec*. 2005;157(4):118.
27. Walsh SR, Linnerth-Petrik NM, Laporte AN, Menzies PI, Foster RA, Wootton SK. Full-length genome sequence analysis of enzootic nasal tumour virus reveals an unusually high degree of genetic stability. *Virus Res*. 2010;151(1):74–87.
28. Yi G, Kaiyu W, QiGui Y, YingDong Y, DeFang C, JinLu H. Pathomorphologic observation of enzootic intranasal adenocarcinoma in Nanjiang yellow goats. *Chin J Vet Sci*. 2010;30(8):1095–7.
29. De las Heras M, de Jalon JG, Minguñon E, Gray E, Dewar P, Sharp J. Experimental transmission of enzootic intranasal tumors of goats. *Vet Pathol*. 1995;32(1):19–23.
30. Langmead B, Trapnell C, Pop M, Salzberg SL. Ultrafast and memory-efficient alignment of short DNA sequences to the human genome. *Genome Biol*. 2009;10(3):R25.
31. Bonneau R, Reiss DJ, Shannon P, Facciotti M, Hood L, Baliga NS, Thorsson V. The Inferelator: an algorithm for learning parsimonious regulatory networks from systems-biology data sets de novo. *Genome Biol*. 2006;7(5):R36.
32. Friedländer MR, Chen W, Adamidi C, Maaskola J, Einspanier R, Knespel S, Rajewsky N. Discovering microRNAs from deep sequencing data using miRDeep. *Nat Biotechnol*. 2008;26(4):407–15.
33. Hofacker IL, Fontana W, Stadler PF, Bonhoeffer LS, Tacker M, Schuster P. Fast folding and comparison of RNA secondary structures. *Monatsh Chem*. 1994;125(2):167–88.
34. Anders S, Huber W. Differential expression analysis for sequence count data. *Genome Biol*. 2010;11(10):R106.
35. Enright AJ, John B, Gaul U, Tuschli T, Sander C, Marks DS. MicroRNA targets in *Drosophila*. *Genome Biol*. 2004;5(1):R1.
36. Kanehisa M, Goto S, Sato Y, Furumichi M, Tanabe M. KEGG for integration and interpretation of large-scale molecular data sets. *Nucleic Acids Res*. 2011;40:D109–14.
37. Carbon S, Ireland A, Mungall CJ, Shu S, Marshall B, Lewis S. AmiGO: online access to ontology and annotation data. *Bioinformatics*. 2009;25(2):288–9.
38. Livak KJ, Schmittgen TD. Analysis of Relative Gene Expression Data Using Real-Time Quantitative PCR and the $2^{-\Delta\Delta CT}$ Method. *Methods*. 2001;25(4):402–8.
39. Rings D, Rojko J. Naturally occurring nasal obstructions in 11 sheep. *Cornell Vet*. 1985;75(2):269–76.
40. De las Heras M, de Jalon JG, Sharp J. Pathology of enzootic intranasal tumor in thirty-eight goats. *Vet Pathol*. 1991;28(6):474–81.
41. Vitellozzi G, Mughetti L, Palmarini M, Mandara M, Mechelli L, Sharp J, Manocchio I. Enzootic intranasal tumour of goats in Italy. *J Veterinary Med Ser B*. 1993;40(1–10):459–68.
42. Ji Z, Wang G, Xie Z, Zhang C, Wang J. Identification and characterization of microRNA in the dairy goat (*Capra hircus*) mammary gland by Solexa deep-sequencing technology. *Mol Biol Rep*. 2012;39(10):9361–71.
43. Yu H, Jun Y. Analysis of miRNAs between 70 Days Fetal and Lamb Skin. *Biotechnology*. 2014;5:018.
44. Chen H, Chen G, Chen Y, Liao W, Liu C, Chang K, Chang Y, Chen S. MicroRNA deregulation and pathway alterations in nasopharyngeal carcinoma. *Br J Cancer*. 2009;100(6):1002–11.
45. Sengupta S, den Boon JA, Chen H-H, Newton MA, Stanhope SA, Cheng Y-J, Chen C-J, Hildesheim A, Sugden B, Ahlquist P. MicroRNA 29c is down-regulated in nasopharyngeal carcinomas, up-regulating mRNAs encoding extracellular matrix proteins. *Proc Natl Acad Sci*. 2008;105(15):5874–8.
46. Xia H, Ng SS, Jiang S, Cheung WK, Sze J, Bian X-W, Kung H-F, Lin MC. miR-200a-mediated downregulation of ZEB2 and CTNBN1 differentially inhibits nasopharyngeal carcinoma cell growth, migration and invasion. *Biochem Biophys Res Commun*. 2010;391(1):535–41.
47. Kano M, Seki N, Kikkawa N, Fujimura L, Hoshino I, Akutsu Y, Chiyomaru T, Enokida H, Nakagawa M, Matsubara H. miR-145, miR-133a and miR-133b: Tumor-suppressive miRNAs target FSCN1 in esophageal squamous cell carcinoma. *Int J Cancer*. 2010;127(12):2804–14.
48. Chiyomaru T, Enokida H, Tatarano S, Kawahara K, Uchida Y, Nishiyama K, Fujimura L, Kikkawa N, Seki N, Nakagawa M. miR-145 and miR-133a function as tumour suppressors and directly regulate FSCN1 expression in bladder cancer. *Br J Cancer*. 2010;102(5):883–91.
49. Iorio MV, Ferracin M, Liu C-G, Veronese A, Spizzo R, Sabbioni S, Magri E, Pedriali M, Fabbri M, Campiglio M. MicroRNA gene expression deregulation in human breast cancer. *Cancer Res*. 2005;65(16):7065–70.
50. Ji H, Wang Z, Perera SA, Li D, Liang M-C, Zaghul S, McNamara K, Chen L, Albert M, Sun Y. Mutations in BRAF and KRAS converge on activation of the mitogen-activated protein kinase pathway in lung cancer mouse models. *Cancer Res*. 2007;67(10):4933–9.
51. Roy S, Jørgensen HG, Roy P, Abed El Baky M, Melo JV, Strathdee G, Holyoake TL, Bartholomew C. BCR-ABL1 tyrosine kinase sustained MECOM expression in chronic myeloid leukaemia. *Br J Haematol*. 2012;157(4):446–56.
52. Pendergast AM, Quilliam LA, Cripe LD, Bassing CH, Dai Z, Li N, Batzer A, Rabun KM, Der CJ, Schlessinger J. BCR-ABL-induced oncogenesis is mediated by direct interaction with the SH2 domain of the GRB-2 adaptor protein. *Cell*. 1993;75(1):175–85.
53. Skorski T, Bellacosa A, Nieborowska-Skorska M, Majewski M, Martinez R, Choi JK, Trotta R, Wlodarski P, Perrotti D, Chan TO. Transformation of hematopoietic cells by BCR/ABL requires activation of a PI-3 k/Akt-dependent pathway. *EMBO J*. 1997;16(20):6151–61.
54. Carlesso N, Frank DA, Griffin JD. Tyrosyl phosphorylation and DNA binding activity of signal transducers and activators of transcription (STAT) proteins in hematopoietic cell lines transformed by Bcr/Abl. *J Exp Med*. 1996;183(3):811–20.
55. Smith DL, Burthem J, Whetton AD. Molecular pathogenesis of chronic myeloid leukaemia. *Expert Rev Mol Med*. 2003;5(27):1–27.
56. Schmidt M, de Mattos SF, van der Horst A, Klompaker R, Kops GJL, Lam EW-F, Burgering BM, Medema RH. Cell cycle inhibition by FoxO forkhead transcription factors involves downregulation of cyclin D. *Mol Cell Biol*. 2002;22(22):7842–52.
57. Martínez-Gac L, Marqués M, García Z, Campanero MR, Carrera AC. Control of cyclin G2 mRNA expression by forkhead transcription factors: novel mechanism for cell cycle control by phosphoinositide 3-kinase and forkhead. *Mol Cell Biol*. 2004;24(5):2181–9.
58. Yuan K, Lian Z, Sun B, Clayton MM, Ng IO, Feitelson MA. Role of miR-148a in hepatitis B associated hepatocellular carcinoma. *PLoS One*. 2012;7(4):e35331.
59. Chen R-H, Miettinen PJ, Maruoka EM, Choy L, Derynck R. A WD-domain protein that is associated with and phosphorylated by the type II TGF- β receptor. *Nature*. 1995;377:548–52.
60. Wu S, Theodorescu D, Kerbel RS, Willson J, Mulder KM, Humphrey LE, Brattain MG. TGF-beta 1 is an autocrine-negative growth regulator of human colon carcinoma FET cells in vivo as revealed by transfection of an antisense expression vector. *J Cell Biol*. 1992;116(1):187–96.
61. Briskin KB, Fady C, Mickel RA, Wang M, Lichtenstein A. Inhibition of head and neck squamous cell carcinoma cell lines by transforming growth factor- β . *Otolaryngol Head Neck Surg*. 1995;112(6):728–34.
62. Arteaga C, Coffey Jr R, Dugger T, McCutchen C, Moses H, Lyons R. Growth stimulation of human breast cancer cells with anti-transforming growth factor beta antibodies: evidence for negative autocrine regulation by transforming growth factor beta. *Cell Growth Differ*. 1990;1(8):367–74.
63. Bin L, Hu C, Zhan F. [The expression in situ of transforming growth factor beta s, their receptors and TGF beta-receptor interacting protein-1 in nasopharyngeal carcinoma]. *Zhonghua Er Bi Yan Hou Ke Za Zhi*. 1999;34(4):210–2.